


Genomic landscape of follicular lymphoma across a wide spectrum of clinical behaviors

Pablo Mozas^{1,2}  | Cristina López^{2,3,4} | Marta Grau² | Ferran Nadeu^{2,3} | Guillem Clot^{2,3,4} | Sara Valle² | Marta Kulis² | Alba Navarro^{2,3} | Joan Enric Ramis-Zaldivar^{2,3} | Blanca González-Farré⁵ | Alfredo Rivas-Delgado¹ | Andrea Rivero¹ | Gerard Frigola^{2,3,5} | Olga Balagué^{2,3,5} | Eva Giné^{1,2,3} | Julio Delgado^{1,2,3,4} | Neus Villamor^{2,3,5} | Estella Matutes⁵ | Laura Magnano^{1,2,3} | Ramón García-Sanz^{3,6} | Sarah Huet^{7,8} | Robert B. Russell⁹ | Elías Campo^{2,3,4,5} | Armando López-Guillermo^{1,2,3,4} | Sílvia Beà^{2,3,4,5} 

¹Department of Hematology, Hospital Clínic de Barcelona, Barcelona, Spain

²Fundació de Recerca Clínic Barcelona-Institut d'Investigacions Biomèdiques August Pi i Sunyer (FRCB-IDIBAPS), Barcelona, Spain

³Centro de Investigación Biomédica en Red de Cáncer (CIBERONC), Madrid, Spain

⁴Departament de Fonaments Clínics, Facultat de Medicina i Ciències de la Salut, Universitat de Barcelona, Barcelona, Spain

⁵Department of Pathology, Haematopathology Section, Hospital Clínic de Barcelona, Barcelona, Spain

⁶Department of Haematology, University Hospital of Salamanca (HUS/IBSAL) and Cancer Research Institute of Salamanca-IBMCC (USAL-CSIC), Salamanca, Spain

⁷Team LIB, ISEM 1111 International Center for Research in Infectiology, Université Claude Bernard Lyon I, Pierre-Bénite, France

⁸France and Department of Biological Haematology, Hôpital Lyon Sud, Hospices Civils de Lyon, Pierre-Bénite, France

⁹Biochemie Zentrum Heidelberg (BZH) and Cell Networks, Bioquant, Ruprecht-Karl University of Heidelberg, Heidelberg, Germany

Correspondence

Sílvia Beà, Pathology Department, Haematopathology Section, Hospital Clínic of Barcelona, Villarroel 170, Esc. 1 Floor -1, Barcelona 08036, Spain.
Email: sbea@clinic.cat

Funding information

Fundación Asociación Española Contra el Cáncer AECC/CIBERONC, Grant/Award Number: PROYE18020BEA; Marató TV3-Cáncer, Grant/Award Number: 201904-30; Generalitat de Catalunya Suport Grups de Recerca AGAUR, Grant/Award Number: 2021-SGR-01293; Fondo de Investigaciones Sanitarias, Instituto de Salud Carlos III, "Cofinanciado por la Unión Europea" and Fondos FEDER: European Regional Development Fund "Una manera de hacer

Abstract

While some follicular lymphoma (FL) patients do not require treatment or experience prolonged responses, others relapse early, and little is known about genetic alterations specific to patients with a particular clinical behavior. We selected 56 grade 1–3A FL patients according to their need of treatment or timing of relapse: never treated ($n = 7$), non-relapsed (19), late relapse (14), early relapse or POD24 (11), and primary refractory (5). We analyzed 56 diagnostic and 12 paired relapse lymphoid tissue biopsies and performed copy number alteration (CNA) analysis and next generation sequencing (NGS). We identified six focal driver losses (1p36.32, 6p21.32, 6q14.1, 6q23.3, 9p21.3, 10q23.33) and 1p36.33 copy-neutral loss of heterozygosity (CN-LOH). By integrating CNA and NGS results, the most frequently altered genes/regions were *KMT2D* (79%), *CREBBP* (67%), *TNFRSF14* (46%) and

Pablo Mozas and Cristina López are Co-first authors.

Armando López-Guillermo and Sílvia Beà are Co-senior authors.

This is an open access article under the terms of the [Creative Commons Attribution](https://creativecommons.org/licenses/by/4.0/) License, which permits use, distribution and reproduction in any medium, provided the original work is properly cited.

© 2023 The Authors. Hematological Oncology published by John Wiley & Sons Ltd.

Europa", Grant/Award Number: PI17/01061; PI19/00887;INT20/00050

BCL2 (40%). Although we found that mutations in *PIM1*, *FOXO1* and *TMEM30A* were associated with an adverse clinical behavior, definitive conclusions cannot be drawn, due to the small sample size. We identified common precursor cells harboring early oncogenic alterations of the *KMT2D*, *CREBBP*, *TNFRSF14* and *EP300* genes and 16p13.3-p13.2 CN-LOH. Finally, we established the functional consequences of mutations by means of protein modeling (*CD79B*, *PLCG2*, *PIM1*, *MCL1* and *IRF8*). These data expand the knowledge on the genomics behind the heterogeneous FL population and, upon replication in larger cohorts, could contribute to risk stratification and the development of targeted therapies.

KEYWORDS

copy number alteration, follicular lymphoma, genomics, next-generation sequencing, prognosis, survival

1 | INTRODUCTION

Survival for patients diagnosed with follicular lymphoma (FL), the most common indolent B cell lymphoma, is now prolonged.¹ However, the continuous pattern of relapses,² early progression³ and histological transformation (HT)⁴ remain current challenges which compromise patients' quantity and quality of life.

FL is characterized by the genetic hallmark t(14;18) (q32;q21), involving the *BCL2* oncogene and the immunoglobulin heavy chain (*IGH*) locus. Deregulation of *BCL2* is an early but not sufficient event driving FL lymphomagenesis.⁵ Additional genetic abnormalities, such as somatic mutations in the chromatin-modifying genes *KMT2D*, *CREBBP*, and *EZH2* are subsequently acquired, with a prominent role in the development, progression, relapse, and HT of FL.^{6–11} Concerning copy number alterations (CNA), losses in 1p36, 6q, 10q, 13q, 17p, and gains in 1q, 2p, 7, 8, 12q, 18q, and trisomy X have been previously associated with prognosis.^{12–14} In an effort to identify higher-risk patients, prognostic indexes have been developed, including clinical or molecular data.¹⁵ Pastore and colleagues developed a prognostic score, the m7-FLIPI,¹⁶ integrating the mutational status of seven genes (*EZH2*, *ARID1A*, *MEF2B*, *EP300*, *FOXO1*, *CREBBP*, and *CARD11*), along with the Follicular Lymphoma International Prognostic index (FLIPI), and Eastern Cooperative Oncology Group (ECOG) performance status. Nonetheless, the m7-FLIPI did not integrate CNA information, which has recently been used to risk-stratify patients independently of clinical parameters.¹⁷ The POD24-PI was devised to predict early relapse by incorporating the mutational status of three genes.¹⁸ Additionally, the gene expression profile of 23 genes (23-GEP score) has also been shown to predict the outcomes of FL patients.¹⁹ However, to date, frontline treatment strategies are not tailored to the result of any of these scores.

Despite the existence of genomic data on FL, the underrepresentation of specific prognostic groups of patients in unselected cohorts hampers the identification of clinically relevant genetic alterations. Here we investigate the genomic abnormalities, using targeted next

generation sequencing (NGS) and CNA, of a total of 56 FL patients categorized into five groups according to their clinical behavior.

2 | PATIENTS AND METHODS

2.1 | Patients

We selected 56 grade 1–3A FL patients diagnosed at a single institution (1997–2015) who met prespecified criteria concerning their need of treatment and timing of relapse (Supplementary Tables S1 and S2). The never treated (NT) group was composed of seven patients who did not require treatment (absence of GELF criteria²⁰) with a minimum follow-up of 5 years (range, 5.4–14.2 years). Nineteen patients were treated with immunochemotherapy (ICT), achieved a complete response, and did not relapse (NR) for at least 10 years of follow-up (range, 11.5–17.8 years). The late relapse (LR) group was made up of 14 patients treated with ICT, who achieved a complete or partial response, and progressed or relapsed beyond two years after frontline treatment (range, 2.1–7 years). Eleven patients were treated with ICT, achieved a complete or partial response, and progressed or relapsed within two years of frontline treatment initiation (early relapse -ER- or POD24³), and five patients were primary refractory (PR) to frontline (immuno)chemotherapy. All patients had an available lymphoid tissue biopsy from the time of diagnosis (D). Additionally, six patients from the LR and six from the ER group had an available biopsy from the first relapse (R).

The study was designed in line with the Declaration of Helsinki and informed consent was obtained according to the Institutional Review Board of Hospital Clínic de Barcelona.²¹

The diagnosis of grade 1–3A FL had been established at the time of consultation and underwent histological review upon inclusion in the study according to the 2017 World Health Organization classification.²² The *BCL2* rearrangement was assessed by polymerase chain reaction (PCR), or fluorescence *in situ* hybridization (FISH)

(Supplementary Figure S1). FISH studies of *BCL6* and *MYC* in relapse samples were performed.

2.2 | Molecular analysis

DNA and RNA from 54 formalin-fixed, paraffin-embedded (FFPE) and two fresh frozen (FF) diagnostic (D) samples, and from 11 FFPE and one FF relapsed (R) samples were extracted using the AllPrep DNA/RNA FFPE Kit (Qiagen, Germany) or the QIAmp DNA/RNA Mini Kit (Qiagen). CNA were analyzed in 56 diagnostic and 12 relapse samples using the Oncoscan CNV FFPE assay (ThermoFisher Scientific). GISTIC was used to identify the targets of focal somatic CNA. The mutational status of 121 genes recurrently altered in B cell lymphoma (Supplementary Table S3) was examined in 55 of 56 diagnostic and 10 of 12 relapse samples (NGS data for diagnostic sample FL027, and relapse samples FL027 and FL034 were not available) using a custom targeted NGS panel and sequenced in a MiSeq instrument (Illumina). The bioinformatic analysis was performed using an updated version of our in-house pipeline^{23,24} (Supplementary Methods).

U1 ribonucleoprotein (U1 small nuclear RNA) mutations were investigated using a custom rhAMP SNP assay (Integrated DNA Technology)²⁵ (Supplementary Table S4). *CDKN2A* DNA methylation status was analyzed using a bisulfite pyrosequencing (BPS) assay (Supplementary Table S5, Supplementary methods). Protein modeling of selected gene variants was performed using the Mechismo²⁶ (Supplementary methods).

The molecular prognostic indexes m7-FLIPI¹⁶ and POD24-PI¹⁸ were calculated according to the original publications. Gene expression profiling (GEP) data was retrieved from patients included in the Huet *et al* study¹⁹ as validation cohort, to calculate their 23-GEP score.

2.3 | Statistical analysis

Quantitative variables were compared among groups by means of ANOVA or Kruskal-Wallis tests. Fisher's exact test was used to compare categorical variables. Statistical significance was defined as a *p* value < 0.05 (Supplementary methods).

3 | RESULTS

3.1 | Baseline features

Baseline and follow-up data of the patients can be found in Table 1 and Supplementary Table S2. Thirty-one patients were female and 25 were male, and median age was 57 years (range, 26–79). Seventy-five percent of patients (42/56) had advanced-stage disease, and 25% had a high-risk FLIPI score. We detected *BCL2* rearrangements in 87% (41/47) of the cases. Among the 48 patients who received treatment during follow-up, 82% were treated with R-CHOP, and the

complete response rate was 83%. With a median follow-up of 12.9 years, 10-year OS was estimated at 79% (95% CI, 69–91).

3.2 | Copy number profile

We analyzed CNA in 56 D and 11 R samples and obtained results in 53 D and 11 R. Alterations were detected in 97% (62/64) of the samples, with a median of 5 alterations (range, 0–26) for diagnostic samples, and of 5 (range, 2–14) for relapse. Considering only D samples, we identified a total of 324 alterations (154 gains, 134 losses, 18 high copy gains, and 18 homozygous deletions) (Figure 1 and Supplementary Table S6) and 89 copy-neutral losses of heterozygosity (CN-LOH).

The most common recurrent alterations (≥ 3 cases) were gains: 1q, 2p16, 12q13-q15, 13q31-q32, 17q22-q24, 18p11-q21, and trisomies 2, 7, 8, 12, 18 and X; losses: 1p36, 6p21, 6q14, 6q23, 9p21, 10q23, 13q14 and 22q13; and CN-LOH: 1p36, 6p25-p21, 12q13 and 16p13. Using GISTIC, we identified six driver losses (*q*-value < 0.05): 1p36.32 (harboring *TNFRSF14*), 6p21.32 (*HLA*), 6q14.1 (*TMEM30A*), 6q23.3 (*TNFAIP3*), 9p21.3 (*CDKN2A/B*), and 10q23.33 (*PTEN*) (Supplementary Table S7). We identified chromothripsis in four patients at diagnosis (4/53, 6%) involving chromosomes 2, 6 and 12, and acquired at relapse in another patient.

3.3 | NGS and integrative analysis

A 121-gene custom targeted sequencing panel was used to analyze 65 FL samples (55 D and 10 R) at a median coverage of 220x (range 12.8x–1417x, Supplementary Table S8), and 98% of the targeted regions at a median coverage of at least 100 reads. We aimed for a minimum coverage of 50x per patient, which led to the exclusion of one sample (FL052). The median number of single-nucleotide variants (SNV) or indels per case was 13 (range 1–32) for diagnostic samples (*n* = 54), and 17 (range 9–22) for relapse samples (*n* = 10) (Supplementary Table S9). We integrated the CNA, SNV, and indels, and identified that the genes/regions altered in >20% at diagnosis were *KMT2D* (79%), *CREBBP* (67%), *TNFRSF14* (46%), *BCL2* (40%), 1p36.33 CN-LOH (27%), *ARID1A* (25%), *TNFAIP3* (23%), *EP300* (21%), 1q gain (21%), trisomy 7 (21%), and 16p13.3–16p13.2 CN-LOH (21%) (Figure 2).

We identified mutations in epigenetic modifier loci (*MEF2B*, *EZH2*, *CREBBP* and *BCL7A*),^{8,16,27,28} genes related to signaling and B cell differentiation (*STAT6* and *POU2AF1*),^{29,30} and the BCR/NF- κ B pathway (*CARD11* and *RRAGC*)³¹ (Supplementary Figure S2). Moreover, we detected recurrently altered genes harboring SNV enriched in target motifs of aberrant somatic hypermutation (*BCL2*, *HIST1H1E*, *TNFRSF14*, *BCL7A* and *OSBPL10*) (Supplementary Table S10). We also explored the U1 snRNA somatic mutations in 51 D and 11 R samples, and identified an acquired mutation only in the R sample of patient FL034 (Supplementary Table S2).

TABLE 1 Salient clinical and genetic features of all the patients of the series, and according to the clinical group.

	All (n = 56)	Never treated (NT, n = 7)	Non-relapsed (NR, n = 19)	Late relapse (LR, n = 14)	Early relapse (ER, n = 11)	Primary refractory (PR, n = 5)
Female sex, n (%)	31 (55)	2 (29)	12 (63)	11 (79)	4 (36)	2 (40)
Median age (range)	57 (26–79)	67 (61–79)	54 (26–74)	61 (26–78)	52 (29–68)	48 (37–73)
ECOG PS ≥ 2 , n (%)	4 (7)	1 (14)	0	1 (7)	0	2 (40)
Ann-Arbor stage III-IV, n (%)	41 (75)	6 (86)	10 (53)	14 (100)	8 (73)	3 (60)
High-risk FLIPI score, n (%)	13 (25)	0	2 (11)	7 (50)	2 (20)	2 (40)
Histological grade 1–2, n (%)	43 (78)	7 (100)	13 (68)	10 (71)	10 (91)	3 (60)
<i>BCL2</i> rearrangement ^a , n (%) [n = 47, 84%]	41 (87)	4 (67)	14 (87)	12 (85)	8 (89)	3 (100)
<i>CARD11</i> mutations, n (%) [n = 54, 96%]	8 (15)	3 (43)	2 (11)	1 (8)	1 (9)	1 (25)
<i>PIM1</i> mutations, n (%) [n = 54, 96%]	6 (11)	0	1 (5)	0	5 (46)	0
High-risk m7-FLIPI score, n (%) [n = 51, 91%]	6 (12)	0	0	2 (15)	2 (20)	2 (67)
High-risk POD24-PI score, n (%) [n = 51, 91%]	12 (24)	0	2 (11)	7 (54)	2 (20)	1 (33)
High-risk 23-GEP score, n (%) [n = 34, 61%]	12 (35)	–	2 (13)	5 (50)	4 (50)	1 (100)
Frontline treatment with R-CHOP, n (%)	45 (82)	–	19 (100)	14 (100)	11 (100)	1 (20) ^c
CR rate, n (%)	40 (83)	–	19 (100)	12 (86)	9 (82)	0
PFS at 5 years, % (95% CI)	47 (34–64)	–	100 (100–100)	31 (14–70)	0	0
OS at 10 years, % (95% CI)	79 (69–91)	71 ^b (45–100)	100	74 (51–100)	82 (62–100)	0

Abbreviations: 23-GEP, 23-gene expression profiling; CI, confidence interval; CR, complete response; ECOG PS, Eastern Cooperative Oncology Group Performance Status; FLIPI, Follicular Lymphoma International Prognostic Index; OS, overall survival; PFS, progression-free survival; POD24-PI, Progression of Disease within 24 months of frontline therapy initiation – Prognostic Index; R-CHOP, rituximab, cyclophosphamide, doxorubicin, vincristine, and prednisone; y, years.

^a*IGH::BCL2* rearrangement by PCR and/or rearranged *BCL2* gene by dual-color, break-apart FISH probe or *IGH::BCL2* dual color dual fusion FISH probe.

^b3 patients from this group died, none of them of lymphoma-related causes (1 unknown cause, 1 lung cancer, 1 hip prosthetic infection).

^cFrontline treatments: CHOP (2), R-CHOP (1), R-bendamustine (1), fludarabine, cyclophosphamide, rituximab (1).

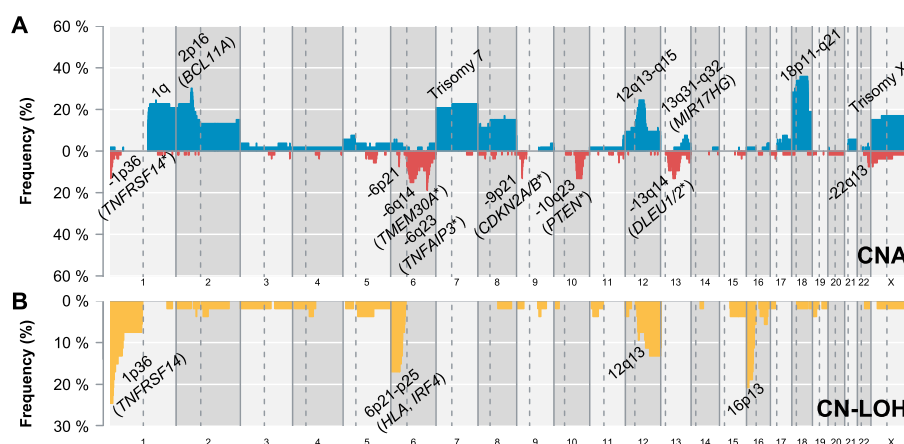


FIGURE 1 Copy number alterations (CNA) of FL samples at diagnosis. Microarray results of the 53 FL patients with data at diagnosis. Panel A depicts the copy number gains (blue), losses (red), and panel B depicts the copy-neutral losses of heterozygosity (CN-LOH) (orange). Each probe is aligned from chromosome 1 to X and from p-arm to q-arm (chromosome Y was excluded). Altered genomic genes/regions relevant for FL pathogenesis are indicated. Driver CNA detected by GISTIC are marked with an asterisk.

We examined the temporal order of genomic alterations in diagnostic samples of FL. We found that the majority of early mutations corresponded to genes related to the epigenome/transcription/translation and proliferation/apoptosis, such as *KMT2D*, *EP300*,

CREBBP, *HIST1H1E*, *BCL7A* and *TNFRSF14* (Supplementary Table S11). In addition, 16p13.3-p13.2 CN-LOH was identified as an early event. In contrast, late aberrations involved genes related to the two abovementioned pathways (*BCL2* and *PIM1*), together with

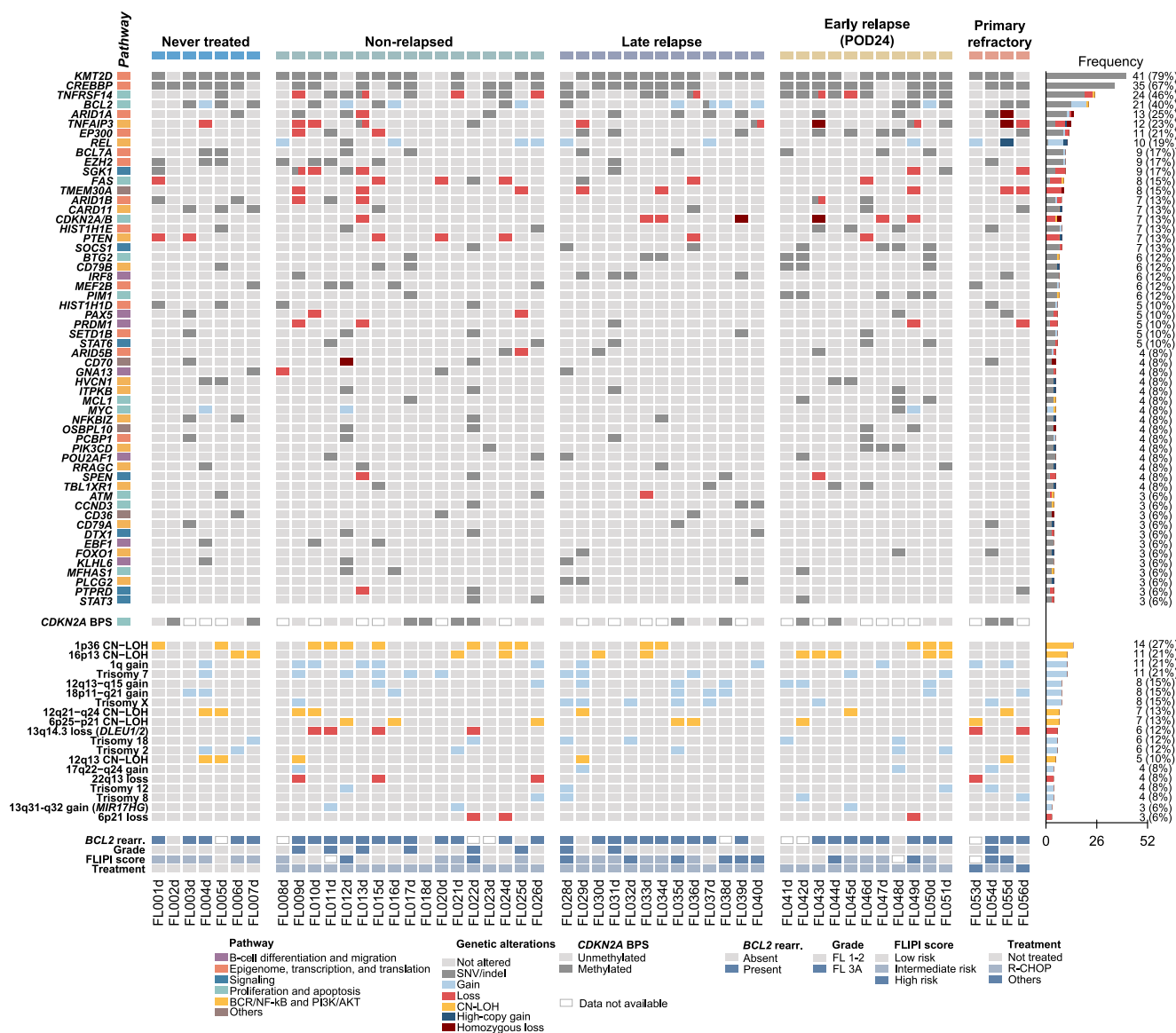


FIGURE 2 Recurrent genomic alterations according to the FL clinical groups. The OncoPrint encompasses the 52 diagnostic samples from the five different clinical groups, analyzed using next generation sequencing and copy number analysis. Altered genes and genomic regions are ordered by decreasing frequency. From top to bottom: single nucleotide variants (SNV), small insertions/deletions (indels) and copy number alterations (CNA) involving specific genes and indicating the pathway (color-coded); bisulfite pyrosequencing (BPS) status of *CDKN2A*, CNA and copy neutral loss of heterozygosity (CN-LOH) and baseline features: *BCL2* rearrangement (*BCL2* rearr.), histological grade, Follicular Lymphoma International Prognostic Index (FLIPI) score, and treatment.

genes related to signaling (*SOCS1*) and the BCR/NF-κB and PI3K/AKT pathways (*CARD11* and *CD79B*). Moreover, chromosomal gains in 1q, 2p16.1 (*REL*) and 18p11.32-q21.33, trisomy 7 and trisomy X were also acquired late in the FL evolution.

We then explored co-occurrence/mutual exclusivity of genetic alterations within the 52 diagnostic samples with available NGS and CNA (Supplementary Figure S3). Aberrations in *FAS* and *PTEN* co-occurred significantly ($Q < 0.05$), and a significant co-occurrence between *PIM1*, *CD79B*, and *BTG2* ($Q < 0.1$) was found, especially in cases that relapsed early (Supplementary Figures S4-S5).

We next investigated the aberrations affecting the genomic region 6q and identified co-occurrence between *PRDM1* and *SGK1* ($Q < 0.05$), between *SGK1* and *TNFAIP3*, *TNFAIP3* and *TMEM30A*, and *TMEM30A* and *PRDM1* ($Q < 0.2$) (Supplementary Figure S6). All the genes located in the 6q region (which were deleted) were also altered by SNV, with the exception of *TMEM30A*. Interestingly, we identified biallelic inactivation of *TNFAIP3* (three cases), and *SGK1* (one case).

We calculated the molecular prognostic indexes for the global series, and the number of patients with a high-risk score was 6 (12%) for m7-FLIPI, 12 (24%) for POD24-PI, and 12 (35%) for 23-GEP.

3.4 | *CDKN2A* methylation status

DNA methylation of CpG islands in *CDKN2A* gene is associated with transcriptional silencing and represents an alternative mechanism to genomic deletion. We used BPS assays and investigated the DNA methylation status of *CDKN2A* promoter in FL cases without 9p21/*CDKN2A* deletions at diagnosis ($n = 42$) or relapse ($n = 5$). We identified *CDKN2A* DNA methylation in 42% of diagnostic samples (13/31). Combining the genomic deletions and the DNA methylation status, we observed that *CDKN2A* was altered in 53% (20/38) of cases (Supplementary Figure S7). None of the four assessable relapse samples harbored *CDKN2A* methylation.

3.5 | Genetic alterations according to the need of treatment and timing of relapse

To elucidate the role of genomic aberrations in FL heterogeneity, we analyzed the prevalence and distribution of altered genes according to their clinical behavior. Although no significant differences were found in the number of SNV/indels or CNA among the five groups, we observed that *CARD11* was more frequently altered in patients who never required treatment compared to those from the other four groups (43 vs. 9%, $p = 0.043$). All the genomic variants identified in *CARD11* were located in the coiled-coil protein domain, essential for the interaction of this cytoplasmic scaffolding protein relevant for NF- κ B activation³² with the paracaspase domain of MALT1.³³

Although we are aware of the limitations of performing survival comparisons among selected groups of patients, we found that *PIM1* mutations were more frequent in early relapse and primary refractory cases ($n = 5$, 33%) than in never-treated, non-relapsed or late relapse cases ($n = 1$, 3%, $p = 0.006$). When only treated patients were considered, there was a trend toward a shorter progression-free survival (PFS) for *PIM1*- [hazard ratio, HR = 2.5 (95% CI 0.9–6.6), $p = 0.07$, Supplementary Figure S8A] and *FOXO1*-mutated cases [HR = 5.5 (95% CI 1.6–19.4), $p = 0.008$, Supplementary Figure S8B]. Univariable Cox regression showed a negative impact on OS for *FOXO1* mutations [HR = 4.9 (95% CI 1.1–22.8), $p = 0.042$, Supplementary Figure S8C], as well as a trend toward a poorer OS for the 8 cases with *TMEM30A* deletion [HR = 2.9 (95% CI 0.9–9.5), $p = 0.076$, Supplementary Figure S8D]. Our dataset was not powered to perform multivariable analyses, due to the low number of cases and the heterogeneity of baseline features.

Regarding the molecular prognostic scores (Table 1), the proportion of patients with a high-risk m7-FLIPI score increased from 0% in NT/NR patients to 15%, 20%, and 67% in LR, ER, and PR patients, respectively ($p = 0.016$). Patients who eventually relapsed (LR/ER/PR, $n = 10$, 53%) were more likely to have a high-risk 23-GEP score at diagnosis than those who did not (NT/NR, $n = 2$, 13%, $p = 0.03$). In our series, the POD24-PI was not significantly different among clinical groups.

3.6 | Clonal evolution

To investigate the clonal evolution of FL, we studied the presence of genetic alterations in the 12 patients with paired samples between D and R. No significant differences were found in the number of SNV/indels or CNA, or in the frequency of specific genes/regions between D and R. We detected a median of 14 shared aberrations (range 5–18). In R samples, a median of 70% of aberrations were shared with D [considering only paired samples analyzed by NGS and CNA ($n = 9$)]. All sample pairs were characterized by the presence of an ancestral common precursor cell (CPC), pointing toward a clonal relationship between the initial and the relapse FL clones (Figure 3A). Besides the shared alterations, we detected additional ones that were unique either to the D or the R sample (Figure 3B), indicating a divergent evolution.

We explored the presence of early alterations in the CPC and found *KMT2D* (7/9), 16p13.3-p13.2 CN-LOH (5/7), *CREBBP* (5/7), *TNFRSF14* (4/9), and *EP300* (3/9) abnormalities. Moreover, analyzing the samples according to the timing of relapse, the late relapse (LR) samples were characterized by *IRF8* mutations in the CPC (Supplementary Figure S9), which were not detected in the CPC of early relapse (ER) samples (Supplementary Figure S10). We also found that the ER group had a percentage of shared aberrations, on average, 13.61 points higher than the LR group (IC 95%: 0.14–27.07, $p = 0.048$) (Supplementary Figure S11). Importantly, although we only identified *TP53* mutations in three ER cases, two of them were acquired upon relapse.

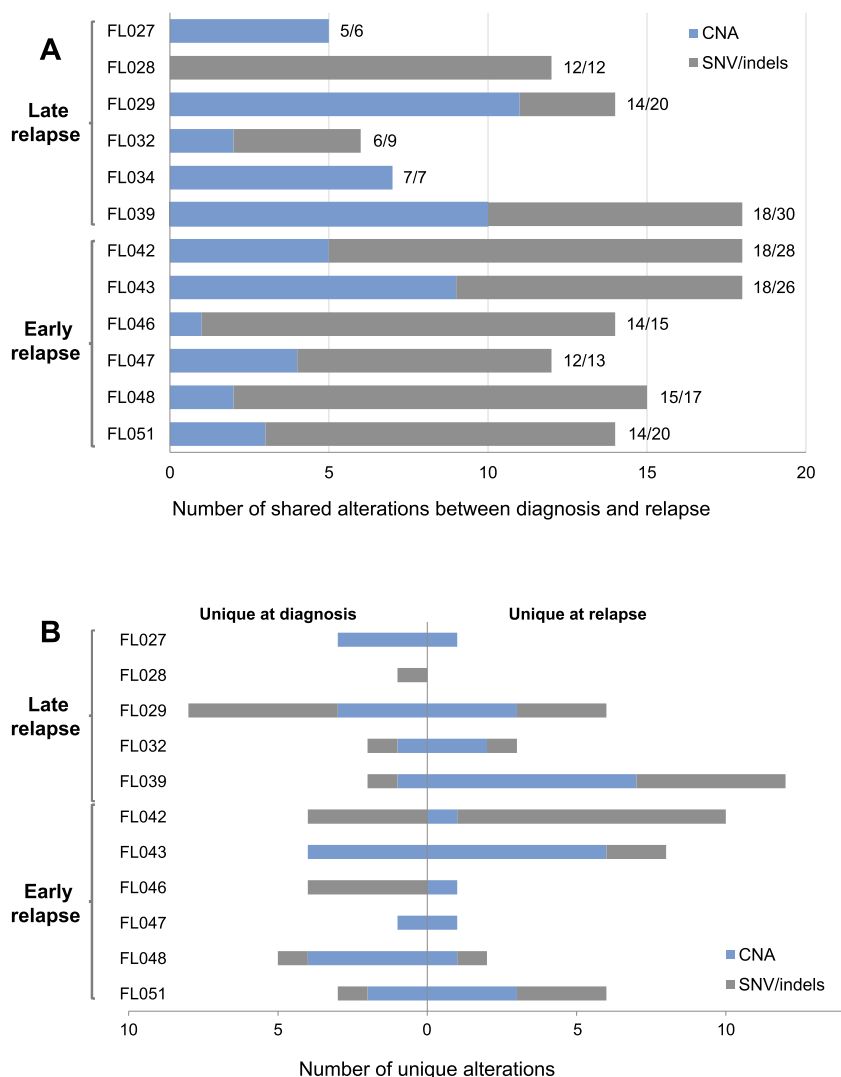
We assessed the presence of *MYC* and *BCL6* translocations by FISH in relapse samples from 10 patients. *BCL6* rearrangements were identified in two samples (FL029 and FL047). In patient FL029, the *BCL6* translocation was already present at diagnosis (FISH for the diagnostic sample of patient FL047 was not available). A *MYC* rearrangement was acquired upon relapse in one patient (FL051) from the ER group.

3.7 | Protein modeling of selected mutations

We modeled proteins encoded by 5 genes relevant to B cell biology, the functional consequences of which have been less explored to date. Three variants in *CD79B* (p.Ile54Arg, 4 cases; p.As118Thr, 1; p. Ala206fs, 1), a protein responsible for mediating immune signals, were detected (Figure 4A). The frameshift variant is predicted to ablate phosphorylation by *src* kinases (e.g., LYN, FYN and BLK)³⁴ leading to abnormal signaling. The two missense variants likely disrupt the extracellular domain responsible for binding CD79A.

Three variants in *PLCG2*, a gene encoding a phospholipase enzyme that is crucial for antigen-stimulated BCR signaling through BTK activation, lie either in the EF-hand region (p.Leu163Phe and p. Pro236Leu) or the C2 domain (p.Thr1152Pro) (Figure 4B), which are close in space, and both domains are involved in the activation of the enzyme.³⁵

FIGURE 3 Total number of shared and unique genomic aberrations identified in FL patients with paired diagnostic/relapse samples, using NGS and CNA analysis. (A), Graph showing the overall shared aberrations in each case, including single nucleotide variants (SNV), indels and copy number aberrations (CNA). (B), Unique genomic aberrations identified at diagnosis and relapse in each case. Note that cases FL027 and FL028 lack NGS and CNA data, respectively, and thus information from those techniques is not displayed. The bar for FL034 is not displayed, since all alterations were shared between diagnosis and relapse.



PIM1 is a proto-oncogene encoding a serine/threonine kinase that has been implicated in many cancers.³⁶ It is itself (auto-)phosphorylated at several sites, which is important for its own activity. Two of the three identified variants (p.Thr114Ile, 4 cases; p.Ser188Asn, 1 case) are immediately adjacent to these sites and thus most likely alter activation. Ser188 and Gln218, are also in regions containing activating mutations in several other kinases (Figure 4C and Supplementary Figure S12A). Similarly, Thr114, lying just N-terminal to the kinase, has some functional resemblance to activating mutations in other kinases (e.g., ZAP70, MAPKAK2/5) where the mutation of such phosphosites leads to constitutive activation.

Two variants in *MCL1*, a member of the Bcl-2 family of proteins involved in the regulation of apoptosis (p.Glu110Gly, 3 cases; p.Leu160Ile, 1), are highly conserved and lie in the PEST region near phosphorylation sites that enhance *MCL1* stability³⁷ (Figure 4D and Supplementary Figure S12B). Both positions likely disrupt the stability and diminish *MCL1* function.

Finally, we found four frameshift and two missense variants in *IRF8* (Figure 4E). The frameshifts were clustered in the C-terminal region of the protein responsible for binding to the SPRY domain

of TRIM21.³⁸ This C-terminal 8 residues resemble the SPRY motif and are predicted by Pepsite³⁹ to bind to the SPRY domain of the IRF8 interactor TRIM21, meaning their loss would abolish this interaction. Frameshifts in this region have been reported previously,⁴⁰ and here they were specific to the LR group. The frameshift variants at this specific region argue for an importance of the specific loss of the IRF4-TRIM21 interaction (Figure 4E). In contrast, missense variants are located in the SMAD domain and likely affect the SMAD domain structure.

4 | DISCUSSION

Although patients diagnosed with FL usually have prolonged survival, their clinical behavior is highly heterogeneous and the ability to stratify FL patients according to their risk at diagnosis is important for predicting their outcome and selecting the most appropriate therapy. In this exploratory study, we assessed the genomic alterations of FL patients according to their need of treatment and duration of response to frontline therapy.

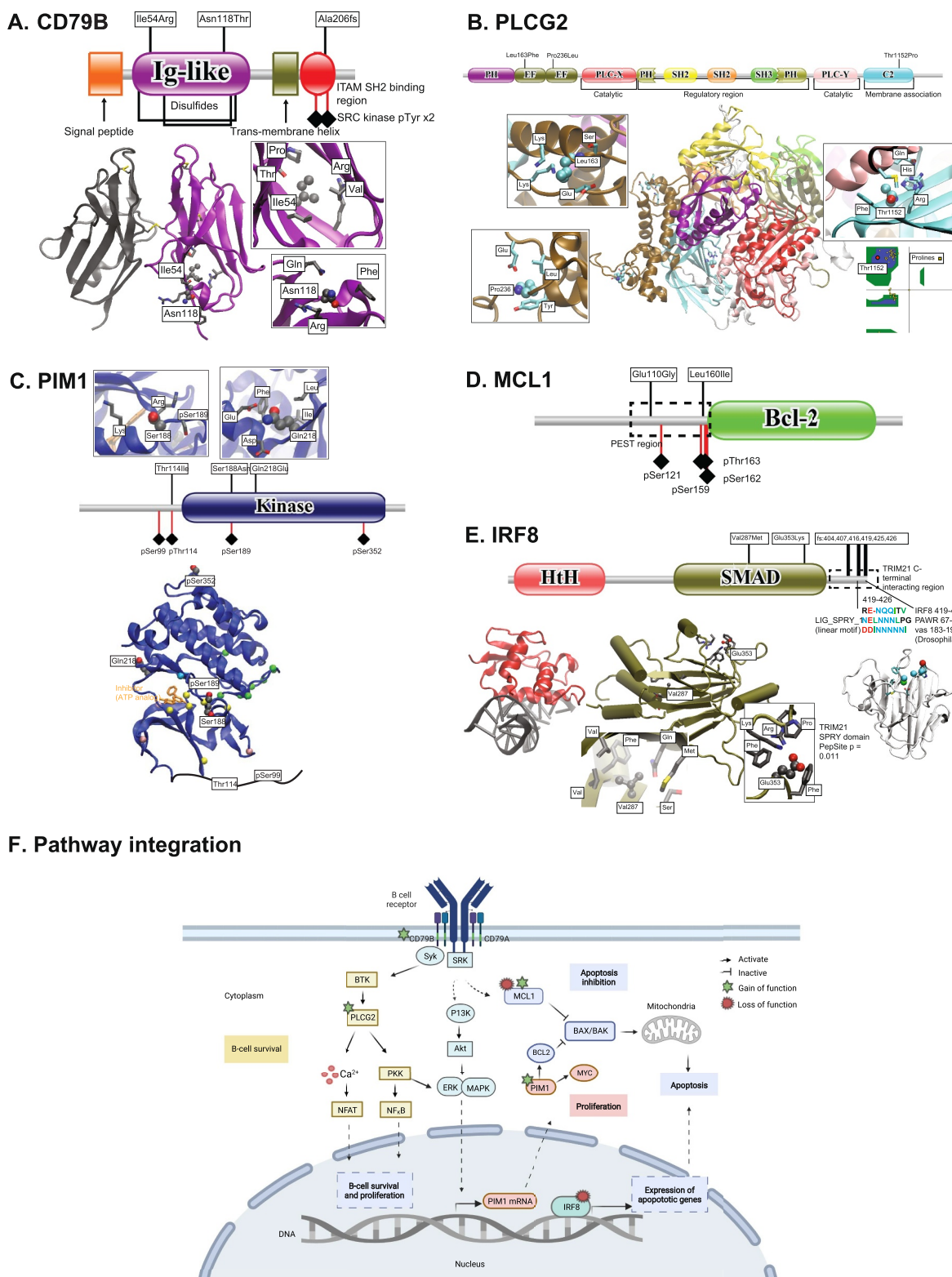


FIGURE 4 Selected protein altering variants on known/predicted structures. (A), Domain schema (top) of human *CD79B* protein showing the location of variants identified in the present study. The schema also shows the location of phosphosites and disulphides below the domains. The structure below shows the dimeric structure of the *CD79B* Immunoglobulin-like domains with the location of the mutated residues as spheres and their interacting residues as sticks. The insets on the right show the regions around the two variants inside this domain. (B), Domain schema (top) of the human *PLCG2* protein showing the location of variants identified. The complete structure of *PLCG2* (modeled based on the *PLCG1* structure PDB:6pbc) and its variants. The inset structures zoom in on the location of specific mutated amino acids (labeled with numbers) and their interacting residues (labeled without numbers). The right bottom figure is a Psi/Phi (Ramachandran) plot showing how the Thr1152 backbone conformation (red circle) compares to those of other prolines in the structure (yellow squares). (C),

In line with previous studies,⁴¹ we found that the FL genetic landscape is characterized by a specific profile of CNA and alterations in genes involved in epigenetic modification, proliferation/apoptosis, and BCR signaling. We identified six focal driver losses and their putative targeted genes affecting 1p36.32 (*TNFRSF14*), 6p21.32 (*HLA*), 6q14.1 (*TMEM30A*), 6q23.3 (*TNFAIP3*), 9p21.3 (*CDKN2A/B*), and 10q23.33 (*PTEN*). These CNA are relevant to the pathogenesis of FL, since losses of *TNFRSF14*, *TNFAIP3* and *CDKN2A/B* have been associated with inferior clinical outcomes and the risk of transformation.^{13,42} On the other hand, evasion of the cytotoxic immune response via *HLA* loss, together with losses of *PTEN* or *TNFAIP3* enhancing PI3K or NF- κ B signaling are important for tumor cell survival.¹²

We also observed that the mutational spectrum changes throughout tumor evolution: certain recurrent alterations in epigenetic modifiers like *KMT2D*, *EP300*, *CREBBP*, *HIST1H1E*, *BCL7A*, and apoptosis genes (e.g., *TNFRSF14*) are early events in disease evolution, in contrast to those in the BCR/NF- κ B and PI3K/AKT (*CARD11* and *CD79B*) and signaling pathways (*SOCS1*), which emerge later. Furthermore, by studying the cases with paired samples, we identified the presence of an ancestral CPC and genomic alterations specific to diagnosis or relapse, suggesting a divergent evolution in all patients. We observed that the cases relapsing early harbored a higher number of shared aberrations than those with a late relapse, corroborating previous findings⁶ describing that early relapses are caused by clones already detected at diagnosis, with only slight clonal dynamic changes.

It must be emphasized that between-group comparisons with a small sample size and testing multiple hypotheses can lead to the identification of false positive findings. That notwithstanding, we found some genetic alterations associated with a specific clinical behavior. *CARD11* mutations were more frequent in patients who never required treatment. This association with a favorable course somewhat contrasts with the adverse prognostic impact attributed to this alteration in the m7-FLIPI study.¹⁶ Explanations for this discrepancy might be multiple: (i) all patients included in the m7-FLIPI study had high tumor burden disease and hence the duration

of watchful waiting was not evaluated, (ii) biopsies in the m7-FLIPI study were obtained within 1 year of treatment initiation, questioning which mutations were present at the time of diagnosis, and (iii) the prognostic impact of some mutations included in the m7-FLIPI score (*ARID1A* and *CARD11*) could not be reproduced in subsequent studies.⁴³

Cases with a short duration of response were enriched in *PIM1* mutations. The biological and clinical impact of *PIM1* alterations has been explored in DLBCL and, more recently, in FL. Crouch et al⁴⁴ identified three molecular clusters in FL: FL_aSHM, FL_STAT6, and FL_Com. Interestingly, the FL_aSHM cluster was enriched in aberrant SHM targets including *DTX1*, *SGK1*, *HIST1H1E*, *BCL7A*, *SOCS1*, *PIM1*, *BTG1*, and *BCL2*, and was associated with a lower overall survival. We detected that *PIM1* alterations co-occurred with those in *CD79B* and *BTG2*, and were more prevalent in patients experiencing an early relapse, indicating a possible role in their aggressive clinical behavior.

According to the recent genetic classifiers for DLBCL,^{45,46} the MCD/C5 subtype is characterized by the co-occurrence of *MYD88*^{L265P} and *CD79B* mutations and is also enriched in *PIM1* and *BTG2* alterations. We may speculate that the association of *CD79B*, *PIM1*, and *BTG2* mutations in our study could be analogous to the MCD/C5 DLBCL subtypes associated with the ABC gene expression subgroup and account for the poor clinical disease course. Despite the co-occurrence of these genomic alterations, we did not find a lower frequency of *BCL2* rearrangement or a lower CD10 expression by immunohistochemistry, which has been postulated as a late germinal center B cell phenotype.^{47,48} The co-occurrence of these genetic alterations may be the result of the chronological hierarchy of oncogenic events in the clonal evolution of FL, or result from sequential rounds of somatic hypermutation, as it has been demonstrated for some aggressive lymphomas.^{44,49} *FOXO1* mutations and *TMEM30A* deletions were associated with decreased survival: *FOXO1* is part of the m7-FLIPI score and associated with a poor prognosis,¹⁶ while deletions of 6q14.1, involving *TMEM30A*, have been associated with inferior prognosis and increased risk of HT.¹³ Our findings are in line with observations in other types of lymphomas^{50,51} and, though preliminary, pave the way for further exploration in larger cohorts.

Domain schema (middle) of the human *PIM1* protein showing the location of variants identified. The schema also shows the location of phosphosites below the domains. The structure to the right (PDB code:3dcv) is that of the catalytic domain and shows the location of Ser97 and Gln127 in addition to the two known phosphosites (pSer89 and pSer261) that lie in this domain. The location of an inhibitor (ATP analog) is also shown in yellow. Positions of known kinase activating mutations are shown as spheres; those lying in the same sequence region as the two *PIM1* variants are shown in yellow; the other colors denote other sequence regions; green variants are in the second major region containing in excess of 5 known activating mutations (from UniProt). (D), Domain schema (top) of the human *MCL1* protein showing the location of variants identified. The schema also shows the location of phosphosites below the domains. (E), Domain schema (top) of the human *IRF8* protein showing the location of variants identified. The bottom left structure is the N-terminal helix-turn-helix (HtH) domain bound to DNA (modeled on mouse *IRF1* PDB:1if1 selected to view the bound DNA). The central structure shows the structure of the SMAD domain (modeled using human *IRF4* PDB:5bvi) and the location of Val287, which sits in a beta-strand region (which is less favored by Met) making mostly hydrophobic contacts, and Glu353, which sits in a pocket close to two positive amino acids (Lys/Arg) making a substitution to Lys unfavorable. The structure on the right shows how the C-terminal 8 amino acids (either containing or near to the six observed frameshifts, fs) are similar to two other peptides known to bind SPRY domains (blue = Asn/Gln; red = Asp/Glu, green = hydrophobic) according to the ELM database. The structure below is the TRIM21 SPRY domain (PDB:2iwig) including the prediction from PepSite³⁹ where the spheres show the predicted location of each amino acid. (F) Schematic representation of the integration of genetic alterations according to biological pathways. Figure (F) created with BioRender.com.

The alterations in *TP53* or *CDKN2A/B*, and *BCL6* or *MYC* translocations have been associated with a more aggressive clinical course in FL⁵² and *CDKN2A* methylation has been described as a mechanism of gene inactivation in various B cell lymphomas, including FL.⁵³ Despite this, we did not identify a particular distribution of these aberrations within the five different clinical groups, which could be due to the limited number of patients and the low prevalence of these alterations in FL diagnostic samples. Herein, we detected that *CDKN2A* methylation changes (42%) were more prevalent than deletions (13%), and observed a trend toward a higher frequency of *CDKN2A/B* deletions in relapsed/refractory cases. Otherwise, we identified the g.3A < C U1 mutation acquired in one FL sample at relapse, and absent in all diagnostic samples, suggesting a possible role in the progression of the disease, albeit further studies are needed to confirm the role of non-coding mutations in FL evolution. It should also be recalled that temporal spatial heterogeneity is a well-recognized phenomenon in FL and therefore the genetic findings originated from a single biopsy site can drastically differ from those from a different area or clinical timepoint. The study of circulating tumor DNA might be an interesting development aiming to capture a pooled representation of the genetic landscape of a tumor.⁵⁴

Selected genes with a relevant role in immune biology (*IRF8*, *PLCG2*, *CD79B*, *PIM1* and *MCL1*), were more thoroughly investigated in order to understand the molecular consequences of the mutations identified in our FL cohort (Figure 4F). *CD79B* mutations have been previously reported in FL.^{7,30,55} The p.Ala206fs found here likely disrupts normal signaling function by preventing phosphorylation by *src* family kinases. This is in line with previous data in ABC DLBCL, which shows increased BCR activity.^{56,57} We found a cluster of *IRF8* C-terminal frameshift variants present in the CPC of cases with a late relapse. The similarity of this region to the SPRY motif suggests that this likely disrupts the interaction with the ubiquitin ligase TRIM21.³⁹ The bulk of evidence indicates that ubiquitination is activating for *IRF8* function,⁵⁸ suggesting that the loss of this C-terminus would lead to a decrease of *IRF8* activity, which is also in line with the molecular consequence predicted for the C-terminal frameshift mutations in DLBCL (cBioPortal, accessed 06/07/2022), and corroborates the association of *IRF8* mutations with a longer time to transformation identified in FL.⁴⁴

According to our modeling analysis the molecular consequence of *PLCG2* variants is a gain of function similar to the previously described in CLL.⁵⁹ Lastly, all *PIM1* variants detected in our study predicted constitutive activation, as described for other kinases,⁶⁰ and enhancing of NF- κ B signaling. *PIM1* has been described as a coactivator of *MYC* promoting tumorigenesis.⁶¹ Although we could not detect a higher incidence of *MYC* alterations in patients with an adverse clinical behavior, *PIM1* somatic mutations were associated with a shorter duration of response and may represent an alternative mechanism of lymphomagenesis.

In conclusion, we confirmed the previously reported CNA and mutations, identified six focal losses as drivers, and established the

temporal order of recurrent alterations in FL. Although the number of patients included in our study is small, we did not identify specific genetic lesions accounting for the diversity of clinical behaviors, pointing to the fact that the heterogeneous clinical course of the disease might be driven by a plethora of genetic lesions, clonal dynamics and microenvironmental interactions.

AUTHOR CONTRIBUTIONS

Pablo Mozas, Cristina López, Armando López-Guillermo and Sílvia Beà designed the study, performed the analysis and wrote the manuscript. Pablo Mozas, Cristina López, Marta Grau, Sara Valle, Marta Kulis, Alba Navarro and Joan Enric Ramis-Zaldivar performed laboratory experiments. Pablo Mozas, Cristina López, Marta Grau, Ferran Nadeu, Guillem Clot, Marta Kulis, Alba Navarro and Joan Enric Ramis-Zaldivar performed bioinformatics analyses. Blanca González-Farré, Gerard Frigola, Olga Balagué and Elías Campo performed histopathological review. Pablo Mozas, Alfredo Rivas-Delgado, Andrea Rivero, Eva Giné, Julio Delgado, Neus Villamor, Estella Matutes, Laura Magnano, Ramón García-Sanz and Armando López-Guillermo provided clinicopathological data. Sarah Huet provided gene expression data. Robert B Russell performed protein modelling studies. All authors contributed to draft writing and approved the final version of the manuscript.

ACKNOWLEDGMENTS

This study was supported by Marató TV3-Cancer (201904-30 to SB), Fundació Associació Espanola Contra el Cancer AECC/CIBERONC: PROYE18020BEA (to SB), Generalitat de Catalunya Suport Grups de Recerca AGAUR (2021-SGR-01293 to S.B.), Fondo de Investigaciones Sanitarias, Instituto de Salud Carlos III, "Cofinanciado por la Unión Europea" and Fondos FEDER: European Regional Development Fund "Una manera de hacer Europa": PI17/01061 (SB), PI19/00887 (ALG and EG), INT20/00050 to AL-G). CL is supported by postdoctoral Beatriz de Pinós grant from Secretaria d'Universitats i Recerca del Departament d'Empresa i Coneixement de la Generalitat de Catalunya and by Marie Skłodowska-Curie COFUND program from H2020 (2018-BP-00055). EC is an Academia Researcher of the "Institució Catalana de Recerca i Estudis Avançats" of the Generalitat de Catalunya. This work was mainly developed at the Centre Esther Koplowitz (CEK), Barcelona, Spain. The authors thank the Hematopathology Collection registered at the Biobank of Hospital Clínic - IDIBAPS for sample procurement. We are indebted to the IDIBAPS Genomics core facility. We are grateful to Miriam Prieto and Silvia Martín for their technical and logistic assistance.

CONFLICTS OF INTEREST STATEMENT

FN has received honoraria from Janssen and AbbVie for speaking at educational activities. EC has been a consultant for Takeda, NanoString, AbbVie and Illumina; has received research support from AstraZeneca, and honoraria from Janssen, EUSPharma and Roche for speaking at educational activities; and is an inventor on a Lymphoma

and Leukemia Molecular Profiling Project patent 'Method for subtyping lymphoma subtypes by means of expression profiling' (PCT/US2014/64161). ALG served on the advisory board of Roche, Celgene, Novartis, and Gilead/Kite and received grants from Celgene, Gilead/Kite.

DATA AVAILABILITY STATEMENT

Next generation sequencing data are available from the European Genome-phenome archive (EGA) under the accession numbers EGAS00001007105.

ORCID

Pablo Mozas  <https://orcid.org/0000-0001-9528-4971>

Silvia Beà  <https://orcid.org/0000-0001-7192-2385>

PEER REVIEW

The peer review history for this article is available at <https://www.webofscience.com/api/gateway/wos/peer-review/10.1002/hon.3132>.

REFERENCES

- Bachy E, Seymour JF, Feugier P, et al. Sustained progression-free survival benefit of rituximab maintenance in patients with follicular lymphoma: long-term results of the PRIMA study. *J Clin Oncol*. 2019;37(31):2815-2824. <https://doi.org/10.1200/JCO.19.01073>
- Rivas-Delgado A, Magnano L, Moreno-Velázquez M, et al. Response duration and survival shorten after each relapse in patients with follicular lymphoma treated in the rituximab era. *Br J Haematol*. 2019;184(5):753-759. <https://doi.org/10.1111/bjh.15708>
- Casulo C, Byrtek M, Dawson KL, et al. Early relapse of follicular lymphoma after rituximab plus cyclophosphamide, doxorubicin, vincristine, and prednisone defines patients at high risk for death: an analysis from the National LymphoCare Study. *J Clin Oncol*. 2015;33(23):2516-2522. <https://doi.org/10.1200/JCO.2014.59.7534>
- Alonso-Álvarez S, Magnano L, Alcoceba M, et al. Risk of, and survival following, histological transformation in follicular lymphoma in the rituximab era. A retrospective multicentre study by the Spanish GELTAMO group. *Br J Haematol*. 2017;178(5):699-708. <https://doi.org/10.1111/bjh.14831>
- Limpens J, Stad R, Vos C, et al. Lymphoma-associated translocation t(14;18) in blood B cells of normal individuals. *Blood*. 1995;85(9):2528-2536. <https://doi.org/10.1182/blood.v85.9.2528.bloodjournal.8592528>
- Kridel R, Chan FC, Mottok A, et al. Histological transformation and progression in follicular lymphoma: a clonal evolution study. *PLoS Med*. 2016;13(12):1-25. <https://doi.org/10.1371/journal.pmed.1002197>
- Okosun J, Bödör C, Wang J, et al. Integrated genomic analysis identifies recurrent mutations and evolution patterns driving the initiation and progression of follicular lymphoma. *Nat Genet*. 2014;46(2):176-181. <https://doi.org/10.1038/ng.2856>
- Pasqualucci L, Khiabani H, Fangazio M, et al. Genetics of follicular lymphoma transformation. *Cell Rep*. 2014;6(1):130-140. <https://doi.org/10.1016/j.celrep.2013.12.027>
- Green MR, Kihira S, Liu CL, et al. Mutations in early follicular lymphoma progenitors are associated with suppressed antigen presentation. *Proc Natl Acad Sci U S A*. 2015;112(10):E1116-E1125. <https://doi.org/10.1073/pnas.1501199112>
- Pasqualucci L, Dominguez-Sola D, Chiarenza A, et al. Inactivating mutations of acetyltransferase genes in B-cell lymphoma. *Nature*. 2011;471(7337):189-196. <https://doi.org/10.1038/nature09730>
- Morin RD, Johnson NA, Severson TM, et al. Somatic mutations altering EZH2 (Tyr641) in follicular and diffuse large B-cell lymphomas of germinal-center origin. *Nat Genet*. 2010;42(2):181-185. <https://doi.org/10.1038/ng.518>
- Bouska A, McKeithan TW, Deffenbacher KE, et al. Genome-wide copy-number analyses reveal genomic abnormalities involved in transformation of follicular lymphoma. *Blood*. 2014;123(11):1681-1690. <https://doi.org/10.1182/blood-2013-05-500595>
- Cheung KJJ, Shah SP, Steidl C, et al. Genome-wide profiling of follicular lymphoma by array comparative genomic hybridization reveals prognostically significant DNA copy number imbalances. *Blood*. 2009;113(1):137-148. <https://doi.org/10.1182/blood-2008-02-140616>
- Johnson NA, Al-Tourah A, Brown CJ, Connors JM, Gascoyne RD, Horsman DE. Prognostic significance of secondary cytogenetic alterations in follicular lymphomas. *Genes Chromosom Cancer*. 2008;47(12):1038-1048. <https://doi.org/10.1002/gcc.20606>
- Mozas P, Rivero A, López-Guillermo A. Past, present and future of prognostic scores in follicular lymphoma. *Blood Rev*. 2021;50:100865. <https://doi.org/10.1016/j.blre.2021.100865>
- Pastore A, Jurinovic V, Kridel R, et al. Integration of gene mutations in risk prognostication for patients receiving first-line immunochemotherapy for follicular lymphoma: a retrospective analysis of a prospective clinical trial and validation in a population-based registry. *Lancet Oncol*. 2015;16(9):1111-1122. [https://doi.org/10.1016/S1470-2045\(15\)00169-2](https://doi.org/10.1016/S1470-2045(15)00169-2)
- Qu X, Li H, Braziel RM, et al. Genomic alterations important for the prognosis in patients with follicular lymphoma treated in SWOG study S0016. *Blood*. 2019;133(1):81-93. <https://doi.org/10.1182/blood-2018-07-865428>
- Jurinovic V, Kridel R, Staiger AM, et al. Clinicogenetic risk models predict early progression of follicular lymphoma after first-line immunochemotherapy. *Blood*. 2016;128(8):1112-1120. <https://doi.org/10.1182/blood-2016-05-717355>
- Huet S, Tesson B, Jais JP, et al. A gene-expression profiling score for prediction of outcome in patients with follicular lymphoma: a retrospective training and validation analysis in three international cohorts. *Lancet Oncol*. 2018;19(4):549-561. [https://doi.org/10.1016/S1470-2045\(18\)30102-5](https://doi.org/10.1016/S1470-2045(18)30102-5)
- Brice P, Bastion Y, Lepage E, et al. Comparison in low-tumor-burden follicular lymphomas between an initial no-treatment policy, prednimustine, or interferon alfa: a randomized study from the Groupe d'Etude des Lymphomes Folliculaires. *J Clin Oncol*. 1997;15(3):1110-1117. <https://doi.org/10.1200/JCO.1997.15.3.1110>
- Hudson TJ, Anderson W, Aretz A, et al. International network of cancer genome projects. *Nature*. 2010;464(7291):993-998. <https://doi.org/10.1038/nature08987>
- Bell D, Gaillard F, IARC. In: *WHO Classification of Tumours of Haematopoietic and Lymphoid Tissues. Revised 4th*; 2010. <https://doi.org/10.5334/rid-9250>
- Nadeu F, Delgado J, Royo C, et al. Clinical impact of clonal and subclonal TP53, SF3B1, BIRC3, NOTCH1, and ATM mutations in chronic lymphocytic leukemia. *Blood*. 2016;127(17):2122-2130. <https://doi.org/10.1182/blood-2015-07-659144>
- Rivas-Delgado A, Nadeu F, Enjuanes A, et al. Mutational landscape and tumor burden assessed by cell-free DNA in diffuse large B-cell lymphoma in a population-based study. *Clin Cancer Res*. 2021;27(2):513-521. <https://doi.org/10.1158/1078-0432.CCR-20-2558>

25. Shuai S, Suzuki H, Diaz-Navarro A, et al. The U1 spliceosomal RNA is recurrently mutated in multiple cancers. *Nature*. 2019;574(7780):712-716. <https://doi.org/10.1038/s41586-019-1651-z>
26. Betts MJ, Lu Q, Jiang Y, et al. Mechismo: predicting the mechanistic impact of mutations and modifications on molecular interactions. *Nucleic Acids Res*. 2015;43(2):e10. <https://doi.org/10.1093/nar/gku1094>
27. Green MR. Chromatin modifying gene mutations in follicular lymphoma. *Blood*. 2018;131(6):595-604. <https://doi.org/10.1182/blood-2017-08-737361>
28. Baliñas-Gavira C, Rodríguez MI, Andrades A, et al. Frequent mutations in the amino-terminal domain of BCL7A impair its tumor suppressor role in DLBCL. *Leukemia*. 2020;34(10):2722-2735. <https://doi.org/10.1038/s41375-020-0919-5>
29. Yildiz M, Li H, Bernard D, et al. Lymphoid neoplasia: activating stat6 mutations in follicular lymphoma. *Blood*. 2015;125(4):668-679. <https://doi.org/10.1182/blood-2014-06-582650>
30. Krysiak K, Gomez F, White BS, et al. Recurrent somatic mutations affecting B-cell receptor signaling pathway genes in follicular lymphoma. *Blood*. 2017;129(4):473-483. <https://doi.org/10.1182/blood-2016-07-729954>
31. Okosun J, Wolfson RL, Wang J, et al. Recurrent mTORC1-activating RRAGC mutations in follicular lymphoma. *Nat Genet*. 2016;48(2):183-188. <https://doi.org/10.1038/ng.3473>
32. Lenz G, Davis RE, Ngo VN, et al. Oncogenic CARD11 mutations in human diffuse large B cell lymphoma. *Science* (80-). 2008;319(5870):1676-1679. <https://doi.org/10.1126/science.1153629>
33. Che T, You Y, Wang D, Tanner MJ, Dixit VM, Lin X. MALT1/Paracaspase is a signaling component downstream of CARMA1 and mediates T cell receptor-induced NF- κ B activation. *J Biol Chem*. 2004;279(16):15870-15876. <https://doi.org/10.1074/jbc.M310599200>
34. Saijo K, Schmedt C, Suhsin I, et al. Essential role of Src-family protein tyrosine kinases in NF- κ B activation during B cell development. *Nat Immunol*. 2003;4(3):274-279. <https://doi.org/10.1038/ni893>
35. Gresset A, Sondek J, Harden TK. The phospholipase C isozymes and their regulation. *Subcell Biochem*. 2015;58:61-94. https://doi.org/10.1007/978-94-007-3012-0_3
36. Mary Photini S, Chaiwangyen W, Weber M, et al. PIM kinases 1, 2 and 3 in intracellular LIF signaling, proliferation and apoptosis in trophoblastic cells. *Exp Cell Res*. 2017;359(1):275-283. <https://doi.org/10.1016/j.yexcr.2017.07.019>
37. Maurer U, Charvet C, Wagman AS, Dejardin E, Green DR. Glycogen synthase kinase-3 regulates mitochondrial outer membrane permeabilization and apoptosis by destabilization of MCL-1. *Mol Cell*. 2006;21(6):749-760. <https://doi.org/10.1016/j.molcel.2006.02.009>
38. Kong HJ, Anderson DE, Lee CH, et al. Cutting edge: autoantigen Ro52 is an interferon inducible E3 ligase that ubiquitinates IRF-8 and enhances cytokine expression in macrophages. *J Immunol*. 2007;179(1):26-30. <https://doi.org/10.4049/jimmunol.179.1.26>
39. Trabuco LG, Lise S, Petsalaki E, Russell RB. PepSite: prediction of peptide-binding sites from protein surfaces. *Nucleic Acids Res*. 2012;40(W1):W423-W427. <https://doi.org/10.1093/nar/gks398>
40. Forbes SA, Beare D, Boutselakis H, et al. COSMIC: somatic cancer genetics at high-resolution. *Nucleic Acids Res*. 2017;45(D1):D777-D783. <https://doi.org/10.1093/nar/gkw1121>
41. Kumar E, Pickard L, Okosun J. Pathogenesis of follicular lymphoma: genetics to the microenvironment to clinical translation. *Br J Haematol*. 2021;194(5):1-12. <https://doi.org/10.1111/bjh.17383>
42. Cheung KJJ, Delaney A, Ben-Neriah S, et al. High resolution analysis of follicular lymphoma genomes reveals somatic recurrent sites of copy-neutral loss of heterozygosity and copy number alterations that target single genes. *Genes Chromosom Cancer*. 2010;49(8):669-681. <https://doi.org/10.1002/gcc.20780>
43. Huet S, Szafer-Glusman E, Xerri L, et al. Evaluation of clinicogenetic risk models for outcome of follicular lymphoma patients in the prima trial. *Hematol Oncol*. 2017;35:96-97. https://doi.org/10.1002/hon.2437_85
44. Crouch S, Painter D, Barrans SL, et al. Molecular subclusters of follicular lymphoma: a report from the UK's Haematological Malignancy Research Network. *Blood Adv*. 2022;6(21):5716-5731. <https://doi.org/10.1182/bloodadvances.2021005284>
45. Chapuy B, Stewart C, Dunford AJ, et al. Molecular subtypes of diffuse large B cell lymphoma are associated with distinct pathogenic mechanisms and outcomes. *Nat Med*. 2018;24(5):679-690. <https://doi.org/10.1038/s41591-018-0016-8>
46. Schmitz R, Wright GW, Huang DW, et al. Genetics and pathogenesis of diffuse large B-cell lymphoma. *N Engl J Med*. 2018;378(15):1396-1407. <https://doi.org/10.1056/nejmoa1801445>
47. Leich E, Salaverria I, Bea S, et al. Follicular lymphomas with and without translocation t(14;18) differ in gene expression profiles and genetic alterations. *Blood*. 2009;114(4):826-834. <https://doi.org/10.1182/blood-2009-01-198580>
48. Horn H, Schmelter C, Leich E, et al. Follicular lymphoma grade 3B is a distinct neoplasm according to cytogenetic and immunohistochemical profiles. *Haematologica*. 2011;96(9):1327-1334. <https://doi.org/10.3324/haematol.2011.042531>
49. Pindzola GM, Razzaghi R, Tavory RN, et al. Aberrant expansion of spontaneous splenic germinal centers induced by hallmark genetic lesions of aggressive lymphoma. *Blood*. 2022;140(10):1119-1131. <https://doi.org/10.1182/blood.2022015926>
50. Hsi ED, Jung SH, Lai R, et al. Ki67 and PIM1 expression predict outcome in mantle cell lymphoma treated with high dose therapy, stem cell transplantation and rituximab: a Cancer and Leukemia Group B 59909 correlative science study. *Leuk Lymphoma*. 2008;49(11):2081-2090. <https://doi.org/10.1080/10428190802419640>
51. Ennishi D, Healy S, Bashashati A, et al. TMEM30A loss-of-function mutations drive lymphomagenesis and confer therapeutically exploitable vulnerability in B-cell lymphoma. *Nat Med*. 2020;26(4):577-588. <https://doi.org/10.1038/s41591-020-0757-z>
52. Pickard L, Palladino G, Okosun J. Follicular lymphoma genomics. *Leuk Lymphoma*. 2020;61(10):2313-2323. <https://doi.org/10.1080/10428194.2020.1762883>
53. Alhajjaily A, Day AG, Feilottter HE, Baetz T, LeBrun DP. Inactivation of the CDKN2A tumor-suppressor gene by deletion or methylation is common at diagnosis in follicular lymphoma and associated with poor clinical outcome. *Clin Cancer Res*. 2014;20(6):1676-1686. <https://doi.org/10.1158/1078-0432.CCR-13-2175>
54. Jiménez-Ubieto A, Poza M, Martín-Muñoz A, et al. Real-life disease monitoring in follicular lymphoma patients using liquid biopsy ultra-deep sequencing and PET/CT. *Leukemia*. 2023;37(3):659-669. <https://doi.org/10.1038/s41375-022-01803-x>
55. Morin RD, Mendez-Lago M, Mungall AJ, et al. Frequent mutation of histone-modifying genes in non-Hodgkin lymphoma. *Nature*. 2011;476(7360):298-303. <https://doi.org/10.1038/nature10351>
56. Davis RE, Ngo VN, Lenz G, et al. Chronic active B-cell-receptor signalling in diffuse large B-cell lymphoma. *Nature*. 2010;463(7277):88-92. <https://doi.org/10.1038/nature08638>
57. Bohers E, Mareschal S, Bouzeflen A, et al. Targetable activating mutations are very frequent in GCB and ABC diffuse large B-cell lymphoma. *Genes Chromosom Cancer*. 2014;53(2):144-153. <https://doi.org/10.1002/gcc.22126>

58. Oke V, Wahren-Herlenius M. The immunobiology of Ro52 (TRIM21) in autoimmunity: a critical review. *J Autoimmun.* 2012;39(1-2):77-82. <https://doi.org/10.1016/j.jaut.2012.01.014>
59. Furman RR, Cheng S, Lu P, et al. Ibrutinib resistance in chronic lymphocytic leukemia. *N Engl J Med.* 2014;370(24):2352-2354. <https://doi.org/10.1056/nejmc1402716>
60. Kuo HP, Ezell SA, Hsieh S, et al. The role of PIM1 in the ibrutinib-resistant ABC subtype of diffuse large B-cell lymphoma. *Am J Cancer Res.* 2016;6(11):2489-2501. <https://doi.org/10.1182/blood.v126.23.699.699>
61. Wang J, Anderson PD, Luo W, Gius D, Roh M, Abdulkadir SA. Pim1 kinase is required to maintain tumorigenicity in MYC-expressing prostate cancer cells. *Oncogene.* 2012;31(14):1794-1803. <https://doi.org/10.1038/onc.2011.371>

SUPPORTING INFORMATION

Additional supporting information can be found online in the Supporting Information section at the end of this article.

How to cite this article: Mozas P, López C, Grau M, et al. Genomic landscape of follicular lymphoma across a wide spectrum of clinical behaviors. *Hematol Oncol.* 2023;41(4):631-643. <https://doi.org/10.1002/hon.3132>